Squalene Based Nanocomposites: A New Platform for the Design of Multifunctional Pharmaceutical Theragnostics

José L. Arias,[†,#] L. Harivardhan Reddy,[‡,#,¶] Mohammad Othman,[#,‡] Brigitte Gillet,[§] Didier Desmaële,[‡] Fatima Zouhiri,[‡] Franco Dosio,[⊥] Ruxandra Gref,[‡] and Patrick Couvreur[‡,*]

[†]Departamento de Farmacia y Tecnología Farmacéutica, Facultad de Farmacia, Universidad de Granada, 18071—Granada, Spain, [‡]Université Paris-Sud XI, Faculté de Pharmacie, UMR CNRS 8612, IFR 141, 92296 Châtenay-Malabry Cedex, France, [§]Université Paris-Sud XI, UMR CNRS 8081, 91405 Orsay Cedex, France, and Laboratoire de Résonance Magnétique Nucléaire Biologique-Institut de Chimie des Substances Naturelles, Gif sur Yvette, France, and [⊥]Università degli Studi di Torino, Facoltà di Farmacia, Dipartimento di Scienza e Tecnologia del Farmaco, 10125 Torino, Italy. [¶] Current address: Sanofi-aventis, 13 Quai Jules-Guesdes 94403 Vitry-sur-Seine, France. [#]These authors contributed equally to this work.

ABSTRACT This study reports the design of a novel theragnostic nanomedicine which combines (i) the ability to target a prodrug of gemcitabine to an experimental solid tumor under the influence of a magnetic field with (ii) the imaging of the targeted tumoral nodule. This concept is based on the inclusion of magnetite nanocrystals into nanoparticles (NPs) constructed by self-assembling molecules of the squalenoyl gemcitabine (SQgem) bioconjugate. The nanocomposites are characterized by an unusually high drug loading, a significant magnetic susceptibility, and a low burst release. When injected to the L1210 subcutaneous mice tumor model, these magnetite/SQgem NPs were magnetically guided, and they displayed considerably greater anticancer activity than the other anticancer treatments (magnetite/SQgem NPs nonmagnetically guided, SQgem NPs, or gemcitabine free in solution). The histology and immunohistochemistry investigation of the tumor biopsies clearly evidenced the therapeutic superiority of the magnetically guided nanocomposites, while Prussian blue staining confirmed their accumulation at the tumor periphery. The superior therapeutic activity and enhanced tumor accumulation has been successfully visualized using T_2-weighted imaging in magnetic resonance imaging (MRI). This concept was further enlarged by (i) the design of squalene-based NPs containing the T_1 Gd^{3+} contrast agent instead of magnetite and (ii) the application to other anticancer squalenoyls, such as, cisplatin, doxorubicin, and paclitaxel. Thus, by combining different anticancer medicines as well as contrast imaging agents in NPs, we open the door toward generic conceptual framework for cancer treatment and diagnosis. This new theragnostic nanotechnology platform is expected to have important applications in cancer therapy.

KEYWORDS: cancer therapy · drug delivery system · magnetic resonance imaging · squalenoyl prodrug · theragnostic nanomedicine · ultrasmall superparamagnetic iron oxide

Cancer is becoming the most frequent cause of death in most developed countries, and in particular the incidence of this disease among women is increasing dramatically. For example, the mortality due to cancer accounts for 23% of the total deaths in the USA,[1] while it represents 31% in men and 19% in women in France.[2]

In spite of the discovery of several potent new therapeutic molecules, the clinical use and efficacy of conventional anticancer agents is still hampered by nonspecific biodistribution and the difficulty of delivering the necessary therapeutic concentration of drug to the tumor site. In some cases, rapid metabolism and clearance contribute to the poor efficacy and/or toxicity of these medicines. Furthermore, drug resistance at the tumor level (noncellular based mechanisms) or at the cellular level (cellular mechanisms) is another major drawback of current chemotherapy.

The introduction of nanotechnology into pharmacology ("nanomedicine") has importantly influenced the drug delivery field, allowing the appearance of new treatments with improved efficacy.[3,4] These nanodevices can be exploited for anticancer therapy as a means to administer the drug into the body in a controlled manner, to deliver it to the tumor,[5,6] and to overcome resistance mechanisms.[7] All of these are challenging objectives. So far, current nanotechnologies for cancer therapy have serious limitations due to the following: (1) poor drug loading which is usually <10% (weight % of the transported drug with respect to the carrier material).[8,9] As a consequence, either the quantity of the anticancer drug administered is not sufficient to reach a pharmacologically active concentration in the body, or the amount of the carrier material to be administered is very high, engendering toxicity or side effects; (2) the rapid release (known as "burst release") of the encapsulated cytotoxic

*Address correspondence to patrick.couvreur@u-psud.fr.

Received for review December 12, 2010 and accepted January 17, 2011.

Published online January 28, 2011
10.1021/nn1034197

compound after administration, generally corresponding to the release within minutes of the fraction of the drug which is simply adsorbed at the surface of the nanocarrier.[10,11] As a result, a significant fraction of the drug will be released before reaching the pharmacological target in the body, leading to poor activity and severe side effects. It has, however, to be noted that some liposomal formulations were already able to reduce the rapid drug release through transmembrane pH gradient; (iii) the difficulty of carrying a sufficient amount of the anticancer drug to the tumor tissue with simultaneous monitoring of the targeting efficiency; and (iv) the complexity of defining easy formulation conditions which can be scaled up in the pharmaceutical industry.

This explains the limited number of marketed nanomedicines, despite the rise of literature in the field. There is, therefore, an urgent need for new ideas able to improve the current way of delivering anticancer compounds for efficient treatment.

In this way, the development of nanotechnologies which combine high drug payloads, targeted anticancer activity, and imaging capabilities ("nanotheragnostics") is of prime interest for scientists in the pharmaceutical world. In recent years, much attention has been paid to the development of magnetic core-based nanoparticles for drug/gene delivery applications,[12,13] taking advantage of the unique ability of magnetic particles to be guided by an applied magnetic field. However, nowadays only few reports in the literature deal with the development of multifunctional drug delivery systems endowed with both magnetic responsiveness and diagnostic imaging capabilities. Studies performed by Gang *et al.*,[14] Yang *et al.*,[15] and Lin *et al.*[16] aiming to develop "nanotheragnostics" deserve to be mentioned. However, most of these studies describe carriers with a magnetic core and polymeric shell, coupled with tumor targeting ligands on the surface.[16] Surprisingly, they were generally focused on the investigation of diagnostic and therapeutic functions independently, and, moreover, were performed *in vitro*, with no clear-cut *in vivo* proof of concept of combined imaging and therapeutic activity.[13,17−22] It is certain that extensive *in vivo* investigations are essential to definitively demonstrate the promise of "nanotheragnostic" as a cutting edge multifunctional platform in cancer therapy.

In this context, we describe here a new concept of nanomedicine with high drug loading and controlled release properties, integrating a theragnostic approach which combines tumor targeting and imaging functionalities. This concept takes advantage of magnetic responsiveness for tumor targeting under the influence of an extracorporeal magnetic field, while the contrast agent property of this system is exploited for MRI imaging. Practically, this multifunctional nanocarrier was prepared by embedding magnetite nanocrystals (USPIO) into a lipophilic prodrug of the anticancer compound gemcitabine (squalenoyl gemcitabine; SQgem, for the synthesis, see Supporting Information, Figure 2a) which has self-assembling properties. We have demonstrated that under the influence of an extracorporeal magnetic field, the intravenously injected magnetic nanomedicine (USPIO/SQgem) was capable of addressing this anticancer compound toward the tumor tissue, where it could be visualized using MRI. The efficacy of this combined approach has been established *in vivo* on an experimental solid tumor model.

This concept has been further enlarged by (i) the design of composite squalene-based NPs containing the T_1 Gd^{3+} contrast agent instead of USPIO (Supporting Information, Figure 2e) and (ii) the application to other categories of anticancer squalenoyl bioconjugates than gemcitabine, that is, the anthracycline doxorubicin (Supporting Information, Figure 2b), the taxoid paclitaxel (Supporting Information, Figure 2c), and the platinum derivative cisplatin (Supporting Information, Figure 2d). By combining different anticancer medicine as well as contrast imaging agents (either T_1 or T_2) in NPs, we open the door toward generic and flexible conceptual framework for cancer treatment and diagnosis.

RESULTS AND DISCUSSION

Particle Geometry, Chemical Composition, And Drug Delivery Properties. Advantageously, the well-stabilized nanomagnetite/squalenoyl antitumor prodrug NPs, such as, nanomagnetite/squalenoyl gemcitabine (USPIO/SQgem), nanomagnetite/squalenoyl doxorubicin (USPIO/SQdox), nanomagnetite/squalenoyl paclitaxel (USPIO/SQptx), and nanomagnetite/squalenoyl cisplatin (USPIO/SQcis) were prepared following a simple one-step nanoprecipitation method (see Supporting Information sections 2.3., 2.4., 2.5., and 2.6). Their size [average diameter (and polydispersity index)] was compatible with parenteral administration: 270 ± 30 nm (and 0.111), 250 ± 25 nm (and 0.127), 265 ± 30 nm (and 0.113), and 245 ± 20 nm (and 0.125), respectively. HRTEM photographs have evidenced that the USPIO particles (see Supporting Information, Figure 1) were completely embedded inside of the squalenoyl antitumor prodrug nanomatrix (Figure 1). The key that enabled us to achieve this successful preparation was clearly the unique spontaneous self-association property of all the squalenoyl prodrug molecules with the USPIO entrapment.

Indeed, almost the entire amount of squalenoyl prodrug used in the preparation method deposited around USPIO (*e.g.,* ∼93% of SQgem, ∼90% of SQdox, ∼87% of SQptx, and ∼91% of SQcis). This led to the formation of nanoparticles (NPs) with extremely high drug loadings compared to the currently available nanocarriers (see Supporting Information section 2.11.2). The efficacy of USPIOs entrapment into squalenoyl anticancer prodrugs was qualitatively confirmed by investigating the electrokinetic properties as well as

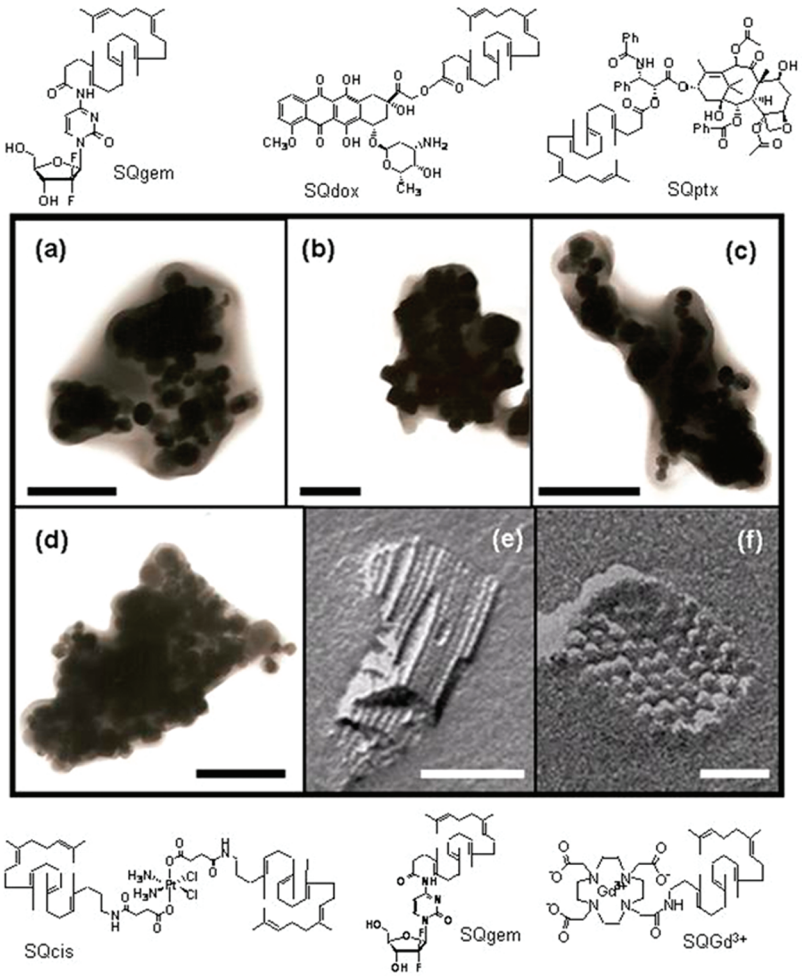

Figure 1. High resolution transmission electron microscopy photographs of USPIO/SQgem (a), USPIO/SQdox (b), USPIO/SQptx (c), and USPIO/SQcis (d) composite (core/shell) NPs. Transmission electron microphotograph after freeze-fracture (FF-TEM) of SQgem NPs (e) and SQgem/SQGd^{3+} composite NPs (f). Bar lengths: 100 nm (a−e), 50 nm (f).

the surface thermodynamics of the nanoparticles (see Supporting Information section 2.11.3). Regarding the release of the squalenoyl prodrugs from the corresponding magnetic core/shell NPs, it was determined that it was quite linear (zero order) during 2 h (see Supporting Information, Figure 10). This period of time may be considered as quite sufficient for the nanocomposites to reach the tumor under the influence of an extracorporeal magnetic field (see Figures 2 and 3, and Supporting Information, Figure 13).

Regarding *in vivo* drug release, it has been previously shown that SQgem nanoparticles did not release gemcitabine in plasma conditions.[23] Cathepsins B and D were identified as the intracellular enzymes responsible for the cleavage of the prodrug leading to gemcitabine release. Pharmacokinetic studies have confirmed that after intravenous administration of SQgem nanoparticles, the major fraction remained in the blood as squalene prodrug.[24] Owing to analytical limitations, it is not easy to highlight at the molecular level the mechanism of drug release *in vivo*. However, as shown previously by Bildstein *et al.*,[25] in tissue culture conditions, SQgem passively diffused into cancer cells and mainly accumulated within cellular membranes, including those of organelles such as the endoplasmic reticulum. SQgem was then released from this transient reservoir into the cell cytoplasm and cleaved into gemcitabine, which either led to the build up of its biologically active triphosphate metabolite, or to gemcitabine efflux through equilibrative membrane transporters. We can expect that similar mechanism occurred with USPIO/SQgem nanocomposite too.

Magnetic Responsiveness. The very good magnetic responsiveness of nanomagnetite/squalenoyl antitumor prodrugs composite nanoparticles was quantitatively investigated by the hysteresis cycle (see Supporting Information, Figure 9a), and qualitatively confirmed by direct observation and microscope visualization of the performance of nanocomposite suspensions under exposure to a 1.1 T permanent magnet (*e.g.*, see Supporting Information, Figure 9b,c of USPIO/SQgem aqueous suspensions).

Visualization of USPIO/SQgem Composites in Solid Tumors Using MRI. Under the influence of an extracorporeal

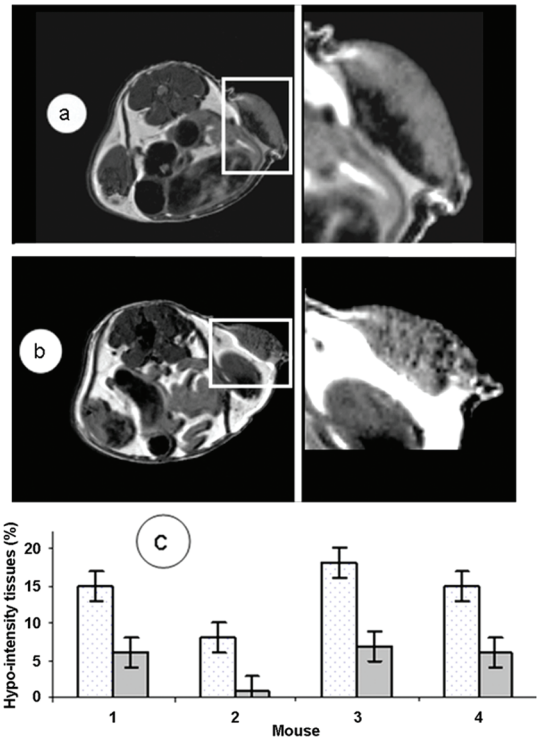

Figure 2. Examples of T_2-weighted images of the tumors obtained at 2 h-postinjection of USPIO/SQgem NPs (a) in the absence of an external magnetic field (mouse 2) and (b) guided by an external magnetic field (1.1 T) (mouse 3); in the latter case, the NPs were found dispersed all over the tumoral tissue. (c) Percentage of the hypo-intensity tissues with T_2 < 36 ms (white column), and with T_2 < 20 ms (gray column). Mouse 2 was injected with nanocomposites without exposition to magnetic field. Mice 1, 3, and 4 were injected with USPIO/SQgem NPs with 2 h exposure to 1.1 T magnetic field.

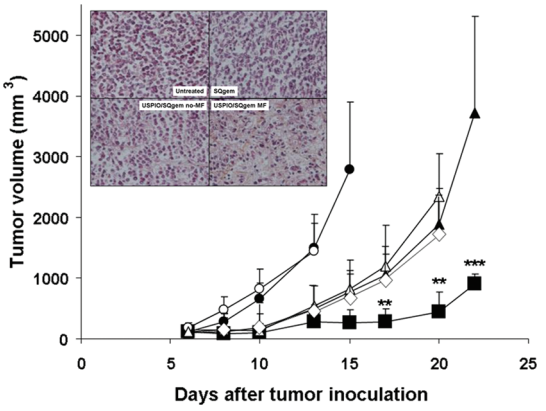

Figure 3. *In vivo* anticancer activity of USPIO/SQgem NPs (with extracorporeal 1.1 T magnetic field) (5 mg/kg equivalent of gemcitabine) compared with placebo-treated group (drug unloaded USPIO/squalene nanocomposites, at same dose and administration schedule as for nanocomposites), USPIO/SQgem NPs (no extracorporeal magnetic field applied) (5 mg/kg equivalent of gemcitabine), with SQgem NPs (5 mg/kg equivalent of gemcitabine), and with gemcitabine free (5 mg/kg) in L1210 subcutaneous tumor bearing mice. Untreated (●), placebo USPIO/squalene NPs (○), gemcitabine (◊), SQgem NPs (▲), USPIO/SQgem composite NPs (no extracorporeal magnetic field) (Δ), USPIO/SQgem composite NPs (with 1.1 T extracorporeal magnetic field) (■). Statistical analysis was performed using Student's *t*-test to compare the statistical significance of USPIO/SQgem composite NPs independently with gemcitabine and SQgem NPs. Data with $**p < 0.05$ and $***p < 0.001$ were considered as significant and very significant, respectively. Inset: Histological examination of tumors isolated from L1210 subcutaneous tumor bearing mice (magnification 40×), untreated or treated either with SQgem NPs (5 mg/kg equivalent of gemcitabine), USPIO/SQgem composites (no extracorporeal magnetic field, no-MF) (5 mg/kg equivalent of gemcitabine), or USPIO/SQgem composites (with 1.1 T extracorporeal magnetic field for 2 h after injection, MF) (5 mg/kg equivalent of gemcitabine).

magnetic field, the intravenously injected magnetic nanomedicine (USPIO/SQgem) was capable of addressing this anticancer compound toward the tumor tissue, where it could be visualized using MRI. Briefly, relaxation time measurements of USPIO/SQgem NPs have shown that they acted as a T_2 and T_2^* contrast agent at 7 T. In the T_2-weighted images registered before intravenous injection of the nanocomposites, the signal in the tumor appeared quite homogeneous, and the mean T_2 relaxation was 46 ± 2 ms. After injection, we observed hypo-intensity areas. This local decrease in intensity corresponded to a T_2 decrease (lower than 36 ms) due to local NP concentration.[26]

To investigate the tumor localization of USPIO/SQgem guided (or not) by an external magnetic field, we measured the tumor volumes and the volumes of the hypo-intensity tissues on 4 animals (see Supporting Information, Figure 11) after injection and placing (or not) during 2 h a 1.1 T magnet onto the tumor nodule. Images of two representative mice and percentage of hypo-intensity tissues in each tumor after injection are shown in Figure 2. Due to variability in tumor growth, the volumes of the nodules were different from mice to mice, but the percentage of hypo-intensity tissue was increased by ≥15% whatever the tumor size when the NPs were guided by the magnetic field. On the contrary, this increase was only 8% when no magnetic field was applied to the tumor. Moreover, the ratio of the least intense region (corresponding to T_2 < 20 ms) drastically increased from 1% to 6%, when the magnetic field was applied. The total amount of nanocomposites distributed into the tumors varied in each case, probably depending on heterogeneity in tumor vascularization. However, when no magnetic field was applied, the hypo-intensity zones appeared only in some slices, and were confined in a part of each slice. On the contrary, the images obtained after the application of a magnetic field showed that the USPIO/SQgem spread out all over the tumor tissue. Thus, *in vivo* MRI experimentation has revealed an improved localization of nanocomposites in tumor nodules when they were guided by an external magnetic field.

Anticancer Activity of USPIO/SQgem Composite Nanoparticles. The anticancer efficacy of USPIO/SQgem has been established on an experimental solid L1210 subcutaneous tumor bearing mice model. Placebo USPIO/squalene NPs injected intravenously (at same dose

and administration schedule as for nanocomposites) did not lead to any antitumor activity. The group of mice treated with USPIO/SQgem but without applying the magnetic field showed a similar response to treatment than that of the mice treated with nonmagnetic SQgem NPs and gemcitabine free. Noteworthy, the administered dose was 20-times lower than the gemcitabine maximum tolerated dose (MTD, 5 mg/kg equiv. gemcitabine vs 100 mg/kg).[27] On the contrary, in the case of mice treated with USPIO/SQgem but whose tumors were exposed to an external magnetic field of 1.1 T (during 2 h postinjection), a considerably greater antitumor activity ($p < 0.05$) was observed, as compared with all the other treatments (Figure 3). Tumor histology examinations further evidence the antitumor activity of magnetic nanocomposites. The histology sections of tumors (inset in Figure 3) clearly demonstrate the superior tumor cell kill effect of the USPIO/SQgem when guided by a 1.1 T magnetic field as indicated by the eradication of a significant tumor cell population, as compared with the tumors of other treatments.

The superiority of magnetically guided USPIO/SQgem NPs in wiping out the proliferating cancer cells from the tumor tissue was demonstrated by performing the K_i-67 cell proliferation assay (see Supporting Information, Figure 12). Furthermore, to support the above observations and to evidence the influence of the extracorporeal magnetic field in guiding the NPs into the tumors, biopsies were analyzed for the differences in the iron accumulation content, using the Prussian blue staining technique. Only the tumor sections of the mice treated with the magnetically guided USPIO/SQgem NPs showed significant accumulation of iron, mainly deposited at the tumor periphery, where the external magnet was placed (see Supporting Information, Figure 13).

Enlargement of the Concept for Cancer Treatment and Diagnosis. In a nutshell, the above observations clearly demonstrated the superiority of this novel concept of magnetically guided NPs for the efficient treatment and imaging of experimental cancer (concretely, solid not operable tumors). This concept has been further enlarged by (i) the design of composite squalene-based NPs containing the T_1 Gd^{3+} contrast agent instead of USPIO (Supporting Information, Figure 2e), and (ii) the application to other categories of anticancer squalenoyl bioconjugates than gemcitabine, that is, the anthracycline doxorubicin (Supporting Information, Figure 2b), the taxoid paclitaxel (Supporting Information, Figure 2c), and the platinum derivative cisplatin (Supporting Information, Figure 2d). A new paradigm in clinical and experimental oncology is a combination therapy involving nanoparticles carrying a combination of drugs. In this respect, the here described nanocomposite particles can potentially deliver a combination of drugs for better therapeutic responses in difficult-to-treat tumors. Additionally, by combining different anticancer medicine as well as contrast imaging agents (either T_1 or T_2) in those composite nanoparticles, we open the door toward generic and flexible conceptual framework for cancer treatment and diagnosis.

To generalize the above concept to other MRI agents, we have investigated a complementary approach to form theragnostics based on the association of the contrast agent gadolinium (Gd^{3+}) with SQgem. The successful coupling of squalene to Gd^{3+} (Supporting Information, Figures 2e and 3) has allowed us to obtain a new derivative, $SQGd^{3+}$, which spontaneously self-assembled in water into the form of micelles of about 7 nm, over a very large concentration range (see Supporting Information section 2.10). The relaxivities of these micelles (Supporting Information, Table 1 and Figure 14) were among the highest values reported in the literature and were about five times higher than the one of the clinically used Dotarem (see Supporting Information, section 2.14.4).[28,29] Noticeably, other lipophilic Gd^{3+} complexes (*e.g.*, cholesterol derivatives) failed to form either micelles or NPs in water, thus, showing lower relaxivities than $SQGd^{3+}$.[30] Moreover, considering the very low critical micelle concentration of $SQGd^{3+}$ (CMC = 9.8 mg/L, see Supporting Information, Figure 4), a great *in vivo* stability of these $SQGd^{3+}$ micelles is hypothesized.

The new $SQGd^{3+}$ contrast agent was further used in association with SQgem to form SQgem/$SQGd^{3+}$ nanoassemblies of ~140 nm (see Figure 1f and Supporting Information section 2.10). Interestingly, the incorporation of $SQGd^{3+}$ to SQgem, even in small amounts, induced dramatic changes in (i) nanoparticle mean diameter and surface charge (see Supporting Information Table S1); and, (ii) the supramolecular organization, as revealed by both X-ray diffraction studies (see Supporting Information section 2.14.2) and TEM after freeze-fracture (Figure 1e,f). Indeed, whereas pure SQgem NPs presented tubular hexagonal-type structures,[31] SQgem/$SQGd^{3+}$ nanocomposites were compact with a regular cubic inner structure (see Supporting Information Figure 14). These observations support the assumption that the $SQGd^{3+}$ and SQgem associated very effectively together in water to form the SQgem/$SQGd^{3+}$ nanocomposites, presumably through strong interactions between their respective lipophilic squalenoyl moieties. Finally, the SQgem/$SQGd^{3+}$ nanocomposites were characterized by high payloads of Gd^{3+} and consequently high relaxivities, comparable to those of $SQGd^{3+}$ (see Table S1).

SUMMARY

This study describes a generic platform to design tumor targeted nanotheragnostics (nanodevices combining anticancer activity and imaging). This new concept takes advantage of the dynamically folded conformation of the natural lipid squalene to build-up

supramolecular assemblies containing both an anticancer squalenoyl prodrug and a MRI agent (ultrasmall particles of iron oxide or gadolinium complex conjugated with squalene). The resulting nanoparticles allow the transport of an unusually high amount of anticancer compounds, without any burst release of the prodrug and with simultaneous visualization of the tumor tissue. When USPIO were used, magnetical guidance became possible, leading to significant anticancer activity. Of course, as previously observed with some other intravenously injected colloids, it has to be verified that adverse reactions will not occur in man (*e.g.*, hypersensitivity).[32] This new "theragnostic" nanotechnology which could be further applied to other medicines than anticancer is expected to have substantial applicability in clinical medicine.

METHODS

General. All these reactions were performed under nitrogen atmosphere unless stated otherwise. Pyridine, triethylamine, toluene, acetonitrile, dichloromethane, and *N,N*-dimethylformamide (DMF) were distilled over calcium hydride, and stored over 4 Å molecular sieves. Ethyl ether and tetrahydrofuran (THF) were distilled from sodium benzophenone ketyl. Analytical thin-layer chromatography was performed on silica gel $60F_{254}$ glass precoated plates (0.25 mm layer) or RP-18 (F_{254}) plates (Merck, Germany). TLC plates were viewed under UV light (254 nm) and visualized with I_2, Kägi-Misher, or Draggendorf reagent. Column chromatography was performed on silica gel 60 (230−400 mesh ASTM) (Merck, Germany). A C-18 reversed-phase 100 silica gel was used for column chromatography of the Gd^{3+} complex (particle size 40−63 μm, surface coverage 17−18%) (Fluka, Switzerland). High resolution transmission electron microscopy (HRTEM) photographs were obtained using a STEM PHILIPS CM20 (The Netherlands) high resolution transmission microscope set at 80 kV accelerating voltage. The ^{1}H and ^{13}C NMR spectra were recorded on Bruker Avance 300 (300 and 75 MHz, for ^{1}H and ^{13}C, respectively) or Bruker Avance 400 (400 and 100 MHz, for ^{1}H and ^{13}C, respectively) spectrometer (USA). Shifts of ^{1}H and ^{13}C NMR spectra were calibrated against the solvent residual peak. Recognition of methyl, methylene, methine, and quaternary carbon nuclei in ^{13}C NMR spectra rests on the *J*-modulated spin−echo sequence. Infrared (IR) spectra were obtained as solid or neat liquid on a Fourier transform Bruker Vector 22 spectrometer (USA). Only significant absorption bands are listed. Low resolution mass spectra (MS) were recorded using electrospray ionization (ESI) conditions in a positive-ion or a negative-ion mode on an Esquire LC Bruker spectrometer (USA). High-resolution mass spectra (HRMS) were recorded using either ESI or MALDI-TOF ionization on a LCT mass spectrometer (Waters, USA) or a Voyager-DE STR mass spectrometer (Applied Biosystems; USA). Elemental analyses were performed with a Perkin-Elmer 2400 analyzer (USA) (Service de microanalyse, Centre d'Etudes Pharmaceutiques, Châtenay-Malabry, France). The gadolinium content in the complex was determined at the Service Central d'Analyze du CNRS (Solaize, France) by inductively coupled plasma atomic emission spectroscopy (ICP-AES) with an ICP-AES, JOBIN YVON spectrometer (China).

Synthesis of Nanomagnetite (USPIO). Nanomagnetite (USPIO) (Supporting Information Figure 1, average diameter and polydispersity index: 9 ± 2 nm and 0.132, respectively) was prepared following the chemical coprecipitation method proposed by Massart[33] (see Supporting Information section 2.2 for further information).

Preparation of Squalenoyl Antitumor Prodrug Nanoparticles and Nanomagnetite/Squalenoyl Antitumor Prodrug Composite Nanoparticles. Synthesis of SQgem nanoassemblies (average diameter and polydispersity index: 110 ± 25 nm and 0.179, respectively) was carried out by nanoprecipitation.[23] Briefly, SQgem was dissolved in ethanol (2 mg/mL) and added dropwise under mechanical stirring (500 rpm, at 25.0 ± 0.5 °C) into a 10^{-5} N HCl aqueous solution, containing pluronic F-68 (1%, w/v) and dextrose (5%, w/v). Under these conditions, the precipitation of SQgem NPs occurred spontaneously. Then, ethanol was evaporated under vacuum at 37.0 ± 0.5 °C using a Buchi Rotavapor (Switzerland) rotary evaporator. NPs were then resuspended in fresh water up to a final volume of 2 mL. The final SQgem aqueous suspensions (2 mg/mL) contained a 5% (w/v) of dextrose and a 1% (w/v) of pluronic F-68. For the characterization experiments, the NPs were freshly prepared and used within 24 h (conservation at 4.0 ± 0.5 °C).

The procedure followed for the synthesis of USPIO/SQgem NPs was similar to that described above for the SQgem NPs, except that SQgem was dissolved in an ethanolic suspension of magnetite nanocrystals (USPIO), prior to nanoprecipitation in water. Practically, SQgem was dissolved in a 0.15% (w/v) USPIO ethanolic suspension (2 mg/mL) and was added dropwise, under mechanical stirring (500 rpm, at 25.0 ± 0.5 °C), to 2 mL of an aqueous medium containing 10^{-5} N HCl, pluronic F-68 (1%, w/v) and dextrose (5%, w/v). Cleaning of the USPIO/SQgem composite NPs was achieved by repeated magnetic separation and redispersion in an aqueous medium containing pluronic F-68 (1%, w/v) and dextrose (5%, w/v), until the supernatant was transparent and its conductivity indicated that the suspensions were clean of both unreacted chemicals and nonmagnetic particles (≤10 μS/cm). For the current investigation, the composite NPs were freshly prepared and used within 24 h (conservation at 4.0 ± 0.5 °C).

Synthesis of SQdox nanoassemblies (average diameter and polydispersity index: 130 ± 20 nm and 0.134, respectively) was done by nanoprecipitation. Briefly, SQdox was dissolved in a mixture of 0.1 mL of ethanol and 0.2 mL of tetrahydrofuran. This solution was added dropwise under mechanical stirring (500 rpm, at 25.0 ± 0.5 °C) into a 10^{-5} N HCl aqueous solution, containing pluronic F-68 (1%, w/v) and dextrose (5%, w/v). Under these conditions, the precipitation of SQdox NPs occurred spontaneously. Then, the organic solvents were evaporated under vacuum at 37.0 ± 0.5 °C using a Buchi Rotavapor (Switzerland) rotary evaporator. NPs were then resuspended in fresh water up to a final volume of 2 mL. The final SQdox aqueous suspensions (2 mg/mL) contained 5% (w/v) dextrose and 1% (w/v) pluronic F-68. For the characterization experiments, the NPs were freshly prepared and used within 24 h (conservation at 4.0 ± 0.5 °C).

The synthesis of USPIO/SQdox NPs was similar to that described above for the SQdox NPs, except that SQdox was dissolved in a 0.15% (w/v) USPIO organic suspension (prepared with 0.1 mL of ethanol and 0.2 mL of tetrahydrofuran), prior to nanoprecipitation in water. This suspension was added dropwise, under mechanical stirring (500 rpm, at 25.0 ± 0.5 °C), to 2 mL of an aqueous medium containing 10^{-5} N HCl, pluronic F-68 (1%, w/v) and dextrose (5%, w/v). Cleaning of the USPIO/SQdox composite NPs was achieved by repeated magnetic separation and redispersion in an aqueous medium containing pluronic F-68 (1%, w/v) and dextrose (5%, w/v), until the supernatant was transparent and its conductivity indicated that the suspensions were clean of both unreacted chemicals and nonmagnetic particles (≤10 μS/cm). For the current investigation, the core/shell NPs were freshly prepared and used within 24 h (conservation at 4.0 ± 0.5 °C).

Synthesis of SQptx nanoassemblies (average diameter and polydispersity index: 140 ± 30 nm and 0.148, respectively) was carried out by nanoprecipitation. Briefly, SQptx was dissolved in ethanol (2 mg/mL) and added dropwise under mechanical stirring (500 rpm, at 25.0 ± 0.5 °C) into a 10^{-5} N HCl aqueous

solution, containing pluronic F-68 (1%, w/v) and dextrose (5%, w/v). Under these conditions, the precipitation of SQptx NPs occurred spontaneously. Then, ethanol was evaporated under vacuum at 37.0 ± 0.5 °C using a Buchi Rotavapor (Switzerland) rotary evaporator. NPs were then resuspended in fresh water up to a final volume of 2 mL. The final SQptx aqueous suspensions (2 mg/mL) contained a 5% (w/v) of dextrose and a 1% (w/v) of pluronic F-68. For the characterization experiments, the NPs were freshly prepared and used within 24 h (conservation at 4.0 ± 0.5 °C).

The procedure followed for the synthesis of USPIO/SQptx NPs was similar to that described above for the SQptx NPs, except that SQptx was dissolved in an USPIO ethanolic suspension, prior to nanoprecipitation in water. Practically, SQptx was dissolved in a 0.15% (w/v) USPIO ethanolic suspension (2 mg/mL) and was added dropwise, under mechanical stirring (500 rpm, at 25.0 ± 0.5 °C), to 2 mL of an aqueous medium containing 10^{-5} N HCl, 1% (w/v) pluronic F-68 and 5% (w/v) dextrose. Cleaning of the USPIO/SQptx NPs was achieved by repeated magnetic separation and redispersion in an aqueous medium containing pluronic F-68 (1%, w/v) and dextrose (5%, w/v), until the supernatant was transparent and its conductivity indicated that the suspensions were clean of both unreacted chemicals and nonmagnetic particles (≤10 μS/cm). For the current investigation, the composite NPs were freshly prepared and used within 24 h (conservation at 4.0 ± 0.5 °C).

Synthesis of SQcis nanoassemblies (average diameter and polydispersity index: 125 ± 15 nm and 0.124, respectively) was done by nanoprecipitation. Briefly, SQcis was dissolved in DMF (2 mg/mL) and added dropwise under mechanical stirring (500 rpm, at 25.0 ± 0.5 °C) into a 10^{-5} N HCl aqueous solution, containing pluronic F-68 (1%, w/v) and dextrose (5%, w/v). Under these conditions, the precipitation of SQcis NPs occurred spontaneously. Then, DMF was removed by dialysis against water with a cellulose ester dialysis membrane (MWco = 500 Da) during 24 h. NPs were then resuspended in fresh water up to a final volume of 2 mL. The final SQcis aqueous suspensions (2 mg/mL) contained a 5% (w/v) of dextrose and a 1% (w/v) of pluronic F-68. For the characterization experiments, the NPs were freshly prepared and used within 24 h (conservation at 4.0 ± 0.5 °C).

The procedure followed for the synthesis of USPIO/SQcis NPs was similar to that described above for the SQcis NPs, except that SQcis was dissolved in a 0.15% (w/v) DMF suspension of USPIO, prior to nanoprecipitation in water. This suspension was added dropwise, under mechanical stirring (500 rpm, at 25.0 ± 0.5 °C), to 2 mL of an aqueous medium containing 10^{-5} N HCl, pluronic F-68 (1%, w/v), and dextrose (5%, w/v). Cleaning of the USPIO/SQcis composite NPs was achieved by repeated magnetic separation and redispersion in an aqueous medium containing pluronic F-68 (1%, w/v) and dextrose (5%, w/v), until the supernatant was transparent and its conductivity indicated that the suspensions were clean of both unreacted chemicals and nonmagnetic particles (≤10 μS/cm). For the current investigation, the nanocomposites were freshly prepared and used within 24 h (conservation at 4.0 ± 0.5 °C) (see Supporting Information sections 2.3, 2.4, 2.5, 2.6, and 2.9 for further details).

Preparation of $SQGd^{3+}$ Micelles and SQgem/$SQGd^{3+}$ Composite Nanoparticles. Remarkably, the newly synthesized $SQGd^{3+}$ contrast agent spontaneously formed micelles (average diameter ≈ 7 nm) in water whatever its concentration (0.1−80 mg/mL). This was achieved by mixing under magnetic stirring the $SQGd^{3+}$ powder in water.

The composite SQgem/$SQGd^{3+}$ NPs were prepared by dissolving 4 mg SQgem in 0.5 mL of a 0.1% (w/v) $SQGd^{3+}$ ethanolic solution. This solution was then added dropwise, under mechanical stirring (500 rpm, at 25.0 ± 0.5 °C) into 1 mL of water. Ethanol was evaporated under vacuum at 37.0 ± 0.5 °C using a Buchi Rotavapor (Switzerland) rotary evaporator. For the characterization experiments, the NPs were freshly prepared and used within 24 h (conservation at 4.0 ± 0.5 °C) (see Supporting Information sections 2.7., 2.8., 2.10., and 2.14 for further details).

Characterization of the Nanomagnetite/Squalenoyl Antitumor Prodrug Composite Nanoparticles. Mean particle diameters were determined in triplicate at 25.0 ± 0.5 °C by photon correlation spectroscopy (PCS) using a Malvern Autosizer 4700 (Malvern Instruments Ltd., UK). The scattering angle was set at 60°, and the measurement was made after suitable dilution of the aqueous nanoparticle suspensions (≈ 0.1%, w/v), that were previously sonicated for 5 min. Using the PCS technique, the instrument evaluates the autocorrelation function of the scattered light intensity; in its standard mode of operation, the software provides an average diameter and a polydispersity index based on the second-order cumulant procedure.

To confirm the size measurements and to carry out a preliminary inspection of the coating efficacy, the size and shape of the NPs (USPIO, SQgem, SQdox, SQptx, SQcis, USPIO/SQgem, USPIO/SQdox, USPIO/SQptx, and USPIO/SQcis) were checked through analysis by high resolution transmission electron microscopy (HRTEM), obtained using a STEM PHILIPS CM20 (The Netherlands) high resolution transmission microscope set at 80 kV accelerating voltage. Prior to observation, dilute suspensions (≈0.1%, w/v) were sonicated for 5 min, and drops were placed on copper grids with Formvar film. The grids were then dried at 35.0 ± 0.5 °C in a convection oven.

The amount of squalenoyl prodrug actually bound to the corresponding USPIO/SQgem, USPIO/SQdox, USPIO/SQptx, and USPIO/SQcis nanocomposite was obtained from the weight difference between the coated nanocomposites and the bare USPIO particles. Drug incorporation to these core/shell NPs was expressed in terms of drug loading (%); for example, gemcitabine loading = (encapsulated gemcitabine (mg)/USPIO/SQgem carrier (mg)) × 100 (see Supporting Information sections 2.11.1., 2.11.2., and 2.11.3 for further details).

Magnetic Properties. The magnetic properties of nanomagnetite and nanomagnetite/squalenoyl antitumor prodrug composite nanoparticles were determined using a Manics DSM-8 vibrating magnetometer (France) at 25.0 ± 0.5 °C. The field-responsive behavior of the nanomagnetite/squalenoyl antitumor prodrug composites was qualitatively analyzed by both optical and microscope visualization of a 0.5% (w/v) aqueous suspension using a 1.1 T permanent magnet close to the flat surfaces of glass vial containing composite particles. Microscope visualization was done using a Nikon SMZ800 (Japan) stereoscopic zoom microscope (see Supporting Information section 2.11.4 for further details).

***In vitro* Squalenoyl Antitumor Prodrug Release from Magnetic Composite Nanoparticles.** SQgem, SQdox, SQptx, and SQcis release from USPIO/SQgem, USPIO/SQdox, USPIO/SQptx, and USPIO/SQgem NPs, respectively, was performed in PBS using the dialysis bag method (pH = 7.4 ± 0.1). The dialysis bag (having a cutoff of 2000 Da (Spectrum Spectra/Por 6 dialysis membrane tubing, USA)) retains the NPs and allows the free squalenoyl prodrug to be released into the dissolution medium. The bags were soaked in water for 12 h before use. Practically, 2 mL of nanomagnetite/squalenoyl antitumor prodrug composites suspension (containing 2 mg/mL of squalenoyl prodrug) was poured into the bag with the two ends fixed by clamps. The bags were placed in a beaker filled with 100 mL of the dissolution medium, and the mixtures were stirred at 200 rpm. The temperature was maintained at 37.0 ± 0.5 °C during all the release experiments, which were performed in triplicate. At different time intervals (0.08, 0.17, 0.25, 0.33, 0.5, 0.75, 1, 2, 3, 6, 9, and 12 h), 5 mL samples of the medium were withdrawn for UV−vis spectrophotometric analysis. An equal volume of PBS solution, maintained at the same temperature, was added after sampling to ensure sink conditions.

UV absorption measurements were carried out in a 8500 UV−vis spectrophotometer (Dinko, Spain) to measure the squalenoyl antitumor prodrug release using quartz cells of 1 cm path length. Good linearity was observed at the maximum absorbance wavelengths, and the method was validated and verified for accuracy, precision and linearity, demonstrating its reproducibility and the absence of molecular interactions. These parameters were studied in standard solutions in six replicates. Noteworthy, no traces of antitumor free drug were observed during the release experiment, showing that no burst release of the free drug occurred during this time interval (see Supporting Information section 2.11.5 for further details).

Visualization of USPIO/SQgem Composites in Solid Tumors Using MRI. Magnetic resonance imaging (MRI) measurements were performed using a horizontal 7 T bore magnet (Oxford, UK) interfaced by an Avance console (Bruker, Germany) and equipped with a 365 mT/m actively shielded gradient device (I.D. = 9 cm, Resonance Research Inc., MA, USA). A 38 mm-diameter birdcage coil was used for transmission and detection (see Supporting Information section 2.12 for further details).

Anticancer Activity of USPIO/SQgem Composite Nanoparticles. The animal experiments were carried out according to the French and European Community guidelines for the care and use of experimental animals. DBA/2 mice (4−5 weeks old) weighing *ca.* 15−18 g were used for this study. The mice were provided with standard mouse food and water *ad libitum*. L1210 wt murine subcutaneous tumor model was developed by subcutaneous injection into the upper part of the right flank of mice, of the exponentially growing L1210 wt leukemia cells (1×10^6 cells) in suspension containing 30% growth factor reduced Matrigel. After waiting for 5 days, when mice developed palpable tumors at the injection site, the mice were randomly divided into six groups of six each, that is, untreated, treated with USPIO/squalene NPs (placebo), treated with gemcitabine (5 mg/kg), treated with SQgem NPs (5 mg/kg equivalent of gemcitabine), treated with USPIO/SQgem NPs (5 mg/kg equivalent of gemcitabine), and treated with USPIO/SQgem NPs under the influence of a 1.1 T extracorporeal magnetic field (5 mg/kg equivalent of gemcitabine). All the groups of tumor bearing mice, except untreated, were intravenously treated on days 6, 9, 13, and 16 after the implantation of tumors (a 4-dose intravenous bolus injection schedule). Following treatment, the mice were monitored regularly for differences in tumor volume reduction to assess the anticancer efficacy (see Supporting Information section 2.13 for further details).

Statistical Analysis. Statistical analysis was performed using Student's *t*-test. Data with $p < 0.05$ and $p < 0.001$ were considered as significant and very significant, respectively.

Acknowledgment. The research leading to these results has received funding from the European research Council under the European Community's Seventh Framework Programme FP7/2007-2013 (Grant Agreement No. 249835). The authors thank Drs. S. L. Mouelhi (Univ. Paris-Sud XI, Chatenay-Malabry, France) for synthesizing the squalenoyl gemcitabine; V. Marsaud and J. M. Renoir (Univ. Paris-Sud XI, Chatenay-Malabry, France) for their help in histology and immunohistochemistry evaluation; S. Laurent, L. van der Elst, and R. N. Muller (Univ. Mons, B-7000 Mons, Belgium) for their help in relaxometric evaluation of the $SQGd^{3+}$; C. Bourgaux (Univ. Paris-Sud XI, Chatenay-Malabry, France) for carrying out X-ray diffractometry studies of the composite nanoparticles; and T. Pouget (LVMH Recherche Parfums et Cosmétiques, Département innovation Matériaux et Technologies, France) for FF-TEM observations. The financial support of the CNRS (Grant "Ingénieur de valorisation of L. H. Reddy, and the associate CNRS researcher fellowship of J. L. Arias) is acknowledged, as well as the Damascus University (Damascus, Syria) for its financial support to M. Othman.

Supporting Information Available: Detailed experimental section [materials; general methods; synthesis of nanomagnetite (USPIO); synthesis of 4-(N)-trisnorsqualenoyl gemcitabine (SQgem); synthesis of 14-trisnorsqualenoyl doxorubicin ester (SQdox); synthesis of 2′-trisnorsqualenoyl paclitaxel ester (SQptx); synthesis of (OC-6−33)-diamminedichlorobis[4-(4,8,13,17,21-pentamethyl-docosa-4,8,12,16,20-pentaenylamino)-4-oxobutanoato]-platinum(IV) (SQcis); synthesis of squalenoyl-DOTA Gd^{3+} complex ($SQGd^{3+}$); determination of the critical micelle concentration (CMC) of the $SQGd^{3+}$ complex; preparation of squalenoyl antitumor prodrug nanoparticles and nanomagnetite/squalenoyl antitumor prodrug composite nanoparticles; preparation of $SQGd^{3+}$ micelles and SQgem/$SQGd^{3+}$ composite nanoparticles; characterization of the nanomagnetite/squalenoyl antitumor prodrug composite nanoparticles (geometry, drug loading, surface electrical and thermodynamic properties, magnetic properties, *in vitro* squalenoyl antitumor prodrug release from magnetic composite nanoparticles); visualization of USPIO/SQgem composites in solid tumors using MRI (*in vivo* MRI protocol, MRI data analysis); anticancer activity of USPIO/SQgem composite nanoparticles (tumor histology and immunohistochemistry studies, determination of USPIO in tumor biopsies of mice treated with USPIO/SQgem nanoparticles); characterization of $SQGd^{3+}$ micelles and SQgem/$SQGd^{3+}$ composite nanoparticles (geometry and surface electrical properties, small-angle X-ray scattering, determination of the amount of $SQGd^{3+}$ in the SQgem/$SQGd^{3+}$ nanocomposites, proton nuclear magnetic relaxation rate analysis); and, statistical analysis], supporting references, supporting Figures S1 to S15, and supporting Table S1. This material is available free of charge *via* the Internet at http://pubs.acs.org.

REFERENCES AND NOTES

1. Official Web site of the American Cancer Society (http://www.cancer.org/docroot/PRO/content/PRO_1_1_Cancer_Statistics_2009_Presentation.asp, accessed December 10, 2010).
2. Official Web site of the Institut National d'Etudes Démographiques (http://www.ined.fr, accessed December 10, 2010).
3. Torchilin, V. P. Multifunctional Nanocarriers. *Adv. Drug Delivery Rev.* **2006,** *58*, 1532–1555.
4. Brigger, I.; Dubernet, C.; Couvreur, P. Nanoparticles in Cancer Therapy and Diagnosis. *Adv. Drug Delivery Rev.* **2002,** *54*, 631–651.
5. Zamboni, W. C. Concept and Clinical Evaluation of Carrier-Mediated Anticancer Agents. *Oncologist* **2008,** *13*, 248–260.
6. Zhang, L.; Gu, F. X.; Chan, J. M.; Wang, A. Z.; Langer, R. S.; Farokhzad, O. C. Nanoparticles in Medicine: Therapeutic Applications and Developments. *Clin. Pharmacol. Ther.* **2008,** *83*, 761–769.
7. Barraud, L.; Merle, P.; Soma, E.; Lefrançois, L.; Guerret, S.; Chevallier, M.; Dubernet, C.; Couvreur, P.; Trépo, C.; Vitvitski, L. Increase of Doxorubicin Sensitivity by Doxorubicin-Loading into Nanoparticles for Hepatocellular Carcinoma Cells *in Vitro* and *in Vivo*. *J. Hepatol.* **2005,** *42*, 736–743.
8. Moog, R.; Burger, A. M.; Brandl, M.; Schüler, J.; Schubert, R.; Unger, C.; Fiebig, H. H.; Massing, U. Change in Pharmacokinetic and Pharmacodynamic Behaviour of Gemcitabine in Human Tumor Xenografts upon Entrapment in Vesicular Phospholipid Gels. *Cancer Chemother. Pharmacol.* **2002,** *49*, 356–366.
9. Yang, J.; Park, S. B.; Yoon, H. G.; Huh, Y. M.; Haam, S. Preparation of Poly ε-Caprolactone Nanoparticles Containing Magnetite for Magnetic Drug Carrier. *Int. J. Pharm.* **2006,** *324*, 185–190.
10. Jiang, B.; Hu, L.; Gao, C.; Shen, J. Ibuprofen-Loaded Nanoparticles Prepared by a Co-precipitation Method and Their Release Properties. *Int. J. Pharm.* **2005,** *304*, 220–230.
11. Esmaeilia, F.; Dinarvand, R.; Ghahremani, M. H.; Ostad, S. N.; Esmaily, H.; Atyabi, F. Cellular Cytotoxicity and *in Vivo* Biodistribution of Docetaxel Poly(lactide-*co*-glycolide) Nanoparticles. *Anticancer Drugs* **2010,** *21*, 43–52.
12. Laurent, S.; Forge, D.; Port, M.; Roch, A.; Robic, C.; Elst, L. V.; Muller, R. N. Magnetic Iron Oxide Nanoparticles: Synthesis, Stabilization, Vectorization, Physicochemical Characterizations, and Biological Applications. *Chem. Rev.* **2008,** *108*, 2064–2110.
13. Shubayev, V. I.; Pisanic, T. R., 2nd; Jin, S. Magnetic Nanoparticles for Theragnostics. *Adv. Drug Delivery Rev.* **2009,** *61*, 467–477.
14. Gang, J.; Park, S. B.; Hyung, W.; Choi, E. H.; Wen, J.; Kim, H. S.; Shul, Y. G.; Haam, S.; Song, S. Y. Magnetic Poly ε-Caprolactone Nanoparticles Containing Fe_3O_4 and Gemcitabine Enhance Anti-Tumor Effect in Pancreatic Cancer Xenograft Mouse Model. *J. Drug Target* **2007,** *15*, 445–453.
15. Yang, X.; Chen, Y.; Yuan, R.; Chen, G.; Blanco, E.; Gao, J.; Shuai, X. Folate-Encoded and Fe_3O_4-Loaded Polymeric Micelles for Dual Targeting of Cancer Cells. *Polymer* **2008,** *49*, 3477–3485.
16. Lin, J. J.; Chen, J. S.; Huang, S. J.; Ko, J. H.; Wang, Y. M.; Chen, T. L.; Wang, L. F. Folic Acid-Pluronic F127 Magnetic Nanoparticle Clusters for Combined Targeting, Diagnosis, and Therapy Applications. *Biomaterials* **2009,** *30*, 5114–5124.

17. McCarthy, J. R.; Jaffer, F. A.; Weissleder, R. A Macrophage-Targeted Theranostic Nanoparticle for Biomedical Applications. *Small* **2006,** *2*, 983–987.
18. Hong, G.; Yuan, R.; Liang, B.; Shen, J.; Yang, X.; Shuai, X. Folate-Functionalized Polymeric Micelle as Hepatic Carcinoma-Targeted, MRI-Ultrasensitive Delivery System of Antitumor Drugs. *Biomed. Microdevices* **2008,** *10*, 693–700.
19. Nasongkla, N.; Bey, E.; Ren, J.; Ai, H.; Khemtong, C.; Guthi, J. S.; Chin, S. F.; Sherry, A. D.; Boothman, D. A.; Gao, J. Multifunctional Polymeric Micelles as Cancer-Targeted, MRI-Ultrasensitive Drug Delivery Systems. *Nano Lett.* **2006,** *6*, 2427–2430.
20. Pan, D.; Caruthers, S. D.; Hu, G.; Senpan, A.; Scott, M. J.; Gaffney, P. J.; Wickline, S. A.; Lanza, G. M. Ligand-Directed Nanobialys as Theranostic Agent for Drug Delivery and Manganese-Based Magnetic Resonance Imaging of Vascular Targets. *J. Am. Chem. Soc.* **2008,** *130*, 9186–9187.
21. Jain, T. K.; Foy, S. P.; Erokwu, B.; Dimitrijevic, S.; Flask, C. A.; Labhasetwar, V. Magnetic Resonance Imaging of Multifunctional Pluronic Stabilized Iron-Oxide Nanoparticles in Tumor-Bearing Mice. *Biomaterials* **2009,** *30*, 6748–6756.
22. Santra, S.; Kaittanis, C.; Grimm, J.; Perez, J. M. Drug/Dye-Loaded, Multifunctional Iron Oxide Nanoparticles for Combined Targeted Cancer Therapy and Dual Optical/Magnetic Resonance Imaging. *Small* **2009,** *5*, 1862–1868.
23. Couvreur, P.; Stella, B.; Reddy, L. H.; Hillaireau, H.; Dubernet, C.; Desmaële, D.; Lepêtre-Mouelhi, S.; Rocco, F.; Dereuddre-Bosquet, N.; Clayette, P.; *et al* Squalenoyl Nanomedicines as Potential Therapeutics. *Nano Lett.* **2006,** *6*, 2544–2548.
24. Reddy, L. H.; Khoury, H.; Paci, A.; Deroussent, A.; Ferreira, H.; Dubernet, C.; Declèves, X.; Besnard, M.; Chacun, H.; Lepêtre-Mouelhi, S.; *et al* Squalenoylation Favorably Modifies the *in Vivo* Pharmacokinetics and Biodistribution of Gemcitabine in Mice. *Drug Metab. Dispos.* **2008,** *36*, 1570–1577.
25. Bildstein, L.; Dubernet, C.; Marsaud, V.; Chacun, H.; Nicolas, V.; Gueutin, C.; Sarasin, A.; Benech, H.; Lepetre-Mouelhi, S.; Desmaële, D.; Couvreur, P. Transmembrane Diffusion of Gemcitabine by a Nanoparticulate Squalenoyl Prodrug: An Original Drug Delivery Pathway. *J. Controlled Release* **2010,** *147*, 163–170.
26. Kastsler, B.; Vetter, D. *Comprendre l'IRM*, 6th ed.; Elsevier Masson S.A.S.: Issy-les Moulineaux, 2006.
27. Reddy, L. H.; Renoir, J. M.; Marsaud, V.; Lepetre-Mouelhi, S.; Desmaële, D.; Couvreur, P. Anticancer Efficacy of Squalenoyl Gemcitabine Nanomedicine on 60 Human Tumor Cell Panel and on Experimental Tumor. *Mol. Pharm.* **2009,** *6*, 1526–1535.
28. Nicolle, G. M.; Tóth, É.; Eisenwiener, K. P.; Mäcke, H. R.; Merbach, A. E. From Monomers to Micelles: Investigation of the Parameters Influencing Proton Relaxivity. *J. Biol. Inorg. Chem.* **2002,** *7*, 757–769.
29. Accardo, A.; Tesauro, D.; Morelli, G.; Gianolio, E.; Aime, S.; Vaccaro, M.; Mangiapia, G.; Paduano, L.; Schillén, K. High-Relaxivity Supramolecular Aggregates Containing Peptides and Gd Complexes as Contrast Agents in MRI. *J. Biol. Inorg. Chem.* **2007,** *12*, 267–276.
30. Oliver, M.; Ahmad, A.; Kamaly, N.; Perouzel, E.; Caussin, A.; Keller, M.; Herlihy, A.; Bell, J.; Miller, A. D.; Jorgensen, M. R. MAGfect: A Novel Liposome Formulation for MRI Labelling and Visualization of Cells. *Org. Biomol. Chem.* **2006,** *4*, 3489–3497.
31. Couvreur, P.; Reddy, L. H.; Mangenot, S.; Poupaert, J. H.; Desmaële, D.; Lepêtre-Mouelhi, S.; Pili, B.; Bourgaux, C.; Amenitsch, H.; Ollivon, M. Discovery of New Hexagonal Supramolecular Nanostructures Formed by Squalenoylation of an Anticancer Nucleoside Analogue. *Small* **2008,** *4*, 247–253.
32. Szebeni, J.; Moghimi, S. M. Liposome Triggering of Innate Immune Responses: A Perspective on Benefits and Adverse Reactions. *J. Liposome Res.* **2009,** *19*, 85–90.
33. Massart, R. Preparation of Aqueous Magnetic Liquids in Alkaline and Acidic Media. *IEEE Trans. Magn.* **1981,** *17*, 1247–1248.